Electronic Supplementary Material (ESI) for Journal of Materials Chemistry
This journal is © The Royal Society of Chemistry 2012

Electronic Supplementary Information for

Radical self-assembled monolayers on Au(111) formed by the adsorption of closed-shell molecules.

Ferdinand Rissner[1,#], ZhongYun Ma[2,3,#], Oliver T. Hofmann[1], Christian Slugovc[4], Zhigang Shuai[5] and Egbert Zojer[1*]

[1] Institute of Solid State Physics, Graz University of Technology, 8010 Graz, Austria

[2] Key Laboratory of Organic Solids, Beijing National Laboratory for Molecular Sciences (BNLMS), Institute of Chemistry, Chinese Academy of Sciences, 100190 Beijing, People's Republic of China

[3] School of Aerospace and Materials Engineering, National University of Defense Technology, 410073 Changsha, People's Repubic of China

[4] Institute for Chemistry and Technology of Materials (ICTM), Graz University of Technology, 8010 Graz, Austria.

[5] Key Laboratory of Organic Opto-Electronics and Molecular Engineering, Department of Chemistry, Tsinghua University, 100084 Beijing, People's Republic of China

[#] These authors have contributed equally to this work.

* egbert.zojer@tugraz.at

This journal is © The Royal Society of Chemistry 2012

S1. Details on the computational methodology

The density-functional theory calculations were performed using the VASP code.[1] Valence electrons were described by a plane-wave basis set (kinetic energy cutoff of approx. 20 Rydberg) and valence-core electron interactions by the projector augmented-wave (PAW) method.[2,3] A 8×5×1 Monkhorst-Pack[4] k-point grid was chosen and a Methfessel-Paxton occupation scheme with a broadening of 0.2eV was used. The metal was modelled by five layers of Au(111) atoms and the resulting unit cell was periodically repeated in all three directions. To exclude spurious interactions between subsequent slabs, a vacuum gap of >20 Å was introduced together with a dipole layer within that vacuum gap to compensate for the asymmetry of the slab. Geometry optimizations were performed using a damped molecular dynamics based scheme until forces fell below 0.01eV/Å. The convergence criterion for electronic relaxations was set to a maximum total energy change of $\Delta E < 1 * 10^{-7}$ eV, which guarantees also a sufficient convergence of the unit cell's dipole moment. During geometry relaxations, the coordinates of the lower three gold layers were fixed (representing the bulk), while the upper two layers (representing the surface) were free to move. Further details regarding the applied computational methodology and the employed parameters are given in ref. [5]. Representations of the systems were generated using XCrysDen.[6] An isovalue of 0.0015 e/A³ was chosen for the LDOS plots and 0.01 a.u. for the orbital plots in Fig. S2.

Van der Waals forces, which are not included in conventional semi-local DFT (density-functional theory) but available via correction schemes[7,8], were not accounted for. This was not considered necessary, as the fundamental electronic changes described in this contribution would be hardly affected by the moderate changes in the tilt- or herringbone-angle such a correction would most likely predict. It would,

This journal is © The Royal Society of Chemistry 2012

however, change the absolute values of the adsorption energies. Considering the overall similarity of the chosen molecules, these changes are expected to be rather similar for each system.

To arrive at a spin-polarised electronic structure, we assumed initial magnetic moments of $1\mu_B$ for all carbon atoms in the unit cell and 0 for the remaining atoms. An antiferromagnetic solution could not be found (using the initial guess of $1\mu_B$ for the carbon atoms of one molecule and $-1\mu_B$ for the carbons of the other molecule). These test calculations converged to the spin-unpolarised solution without magnetization. We note that reducing the Methfessel-Paxton smearing from 0.2 eV to 0.00862 eV (100 K) gave the same magnetic moments for the systems with molecules **1** and **3**, while for **2** a value of 0.78 μ_B instead of the reported 1.55 μ_B was found.

The bond lengths used to produce Fig. 3 and Fig. S4 were calculated considering the average values of equivalent bonds (ignoring the minor deviations due to the fact that, strictly speaking, no symmetry-equivalent bonds exist in these molecules). In the adsorbed layers, averaging was done over both molecules in the unit cell.

S2. Dependence of the spin-splitting in the isolated molecule 1 on the chosen exchange-correlation functional.

It is well known that semi-local DFT calculations underestimate the gap of semiconductors, and hybrid functionals usually increase the gap compared to the semi-local result.[9] As discussed in the main text,

This journal is © The Royal Society of Chemistry 2012

after adsorption of molecules **1**-**3**, the relevant gap is the difference between α- and β-channel of the SOMO (singly occupied molecular orbital)-derived band. While hybrid calculations can be easily done for open boundary conditions, they are computationally demanding in periodic systems. Calculating the complete metal/SAM interface using a hybrid functional is a quite formidable task that we have recently mastered for closed-shell SAMs,[10] but we have not yet succeeded for spin-polarised calculations and are also not aware that anyone else has. Because of this, we only tested the dependence of the α-HOMO/β-LUMO gap for the gas phase radical derived from **1**. It was obtained by reducing the thiocarbonyl group with atomic hydrogen (see Fig. S2). The resulting α-HOMO and β-LUMO are shown in Fig. S2 and the LDA, GGA and B3LYP gap are given. While for all functionals both orbitals are reminiscent of the closed-shell LUMO (see Fig. S3), the gap is strongly dependent on the chosen functional, changing by almost 1.5eV between LDA and B3LYP.

It is, however, far from trivial to transfer this functional-dependence of the gap to the calculations of the adsorbed monolayer presented in the main text, as in the latter situation the molecular electronic structure is severely modified. The two main reasons for this are the dielectric screening in the monolayer due to the neighboring molecules and the screening by the nearby metal.[11,12,13] Both effects reduce the band gap, and both effects are missed by semi-local as well as hybrid functionals. Because of this, the error of the results presented in the main text (using the semi-local PW91 functional) is most likely smaller than the data in Fig. S2 suggests.

This journal is © The Royal Society of Chemistry 2012

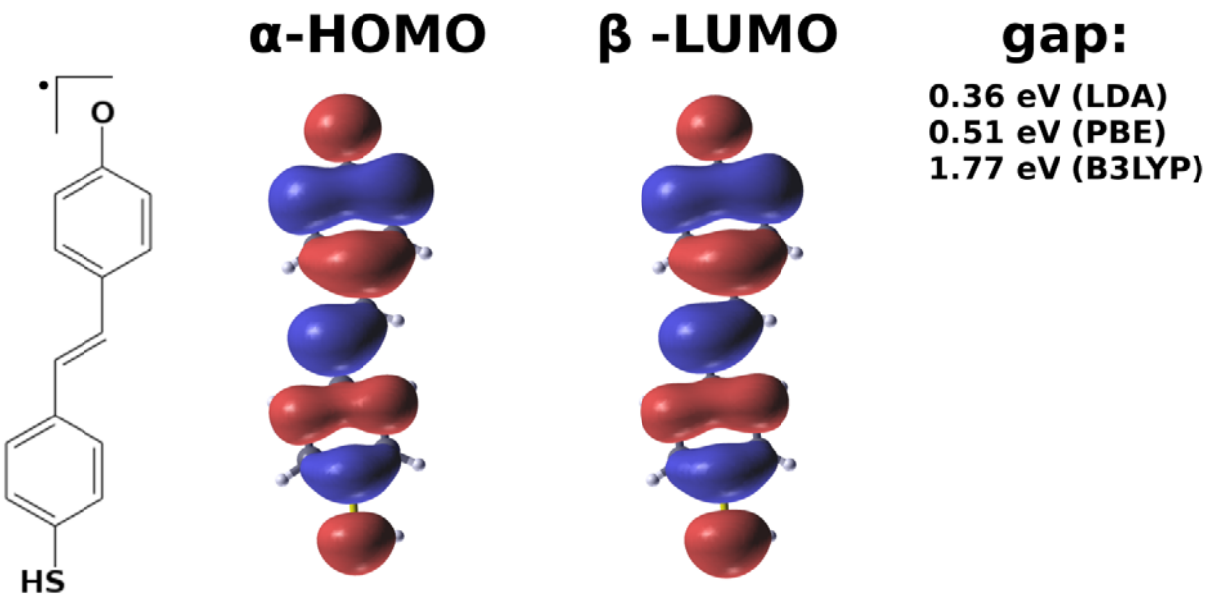

*Fig. S2. Gas phase radical derived from molecule **1** (see Fig. 1 in the main text) by addition of a hydrogen atom, its α-HOMO and β-*LUMO and the related gap for different functionals.

S3. Comparison of LDOS representations in the adsorbed monolayer with gas phase data.

The LDOS plots in energy windows of 0.1eV below and above the Fermi energy E_F shown in Fig. 2 in the main text for the adsorbed monolayer of **1** is reproduced in Fig. S3 together with the equivalent data for **2**, **3** and **1t**. In addition, Fig. S3 shows the LDOS of the gas phase π-HOMO[1] and LUMO orbitals of these molecules. It can be seen that only in case of **1t** the states near E_F are derived from the π-HOMO, whereas in all other systems these states are reminiscent of the LUMO.

[1] Note that in the PW91 calculations of the isolated molecules, a localized σ-orbital is found as HOMO and the delocalized π-orbital is only the HOMO-1. This is not the case in calculations using a hybrid functional, which can be rationalized as an orbital-dependent self-interaction error in the PW91 calculation.[14,10]

This journal is © The Royal Society of Chemistry 2012

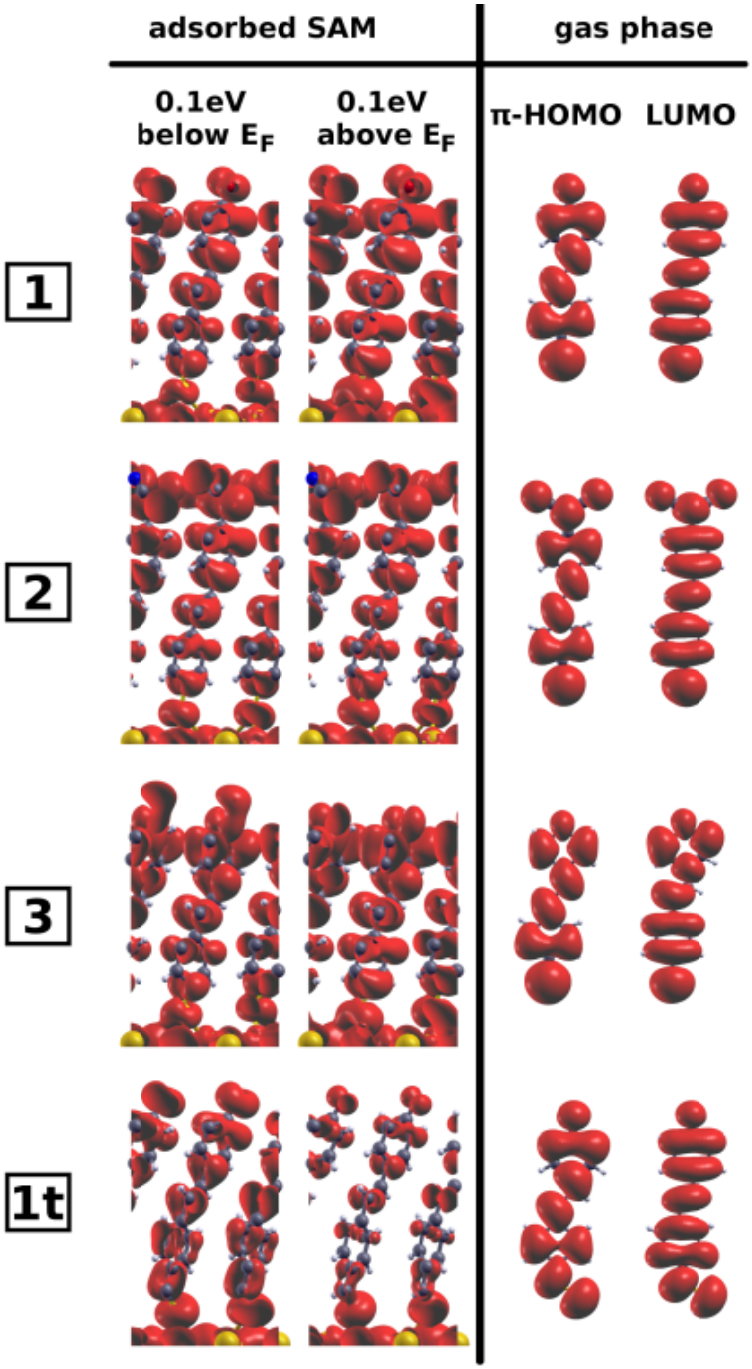

*Fig. S3. LDOS plots in energy windows of 0.1eV below and above the Fermi energy E_F for the adsorbed monolayers of molecules **1**, **2**, **3** and **1t**. In addition, the LDOS of the respective gas phase π-HOMO and LUMO orbitals is shown.*

This journal is © The Royal Society of Chemistry 2012

S4. Bond length changes upon adsorption of 1 on the Au(111) surface, and subsequent reduction.

Upon adsorption of **1**, the molecular backbone changes from a quinoidal towards an aromatic structure. This is evident from the bond length changes shown in Fig. S4. Significant values are found below the upper ring. The backbone is further pushed towards an aromatic structure upon reduction on the surface, where the largest bond length modifications are found above the lower ring.

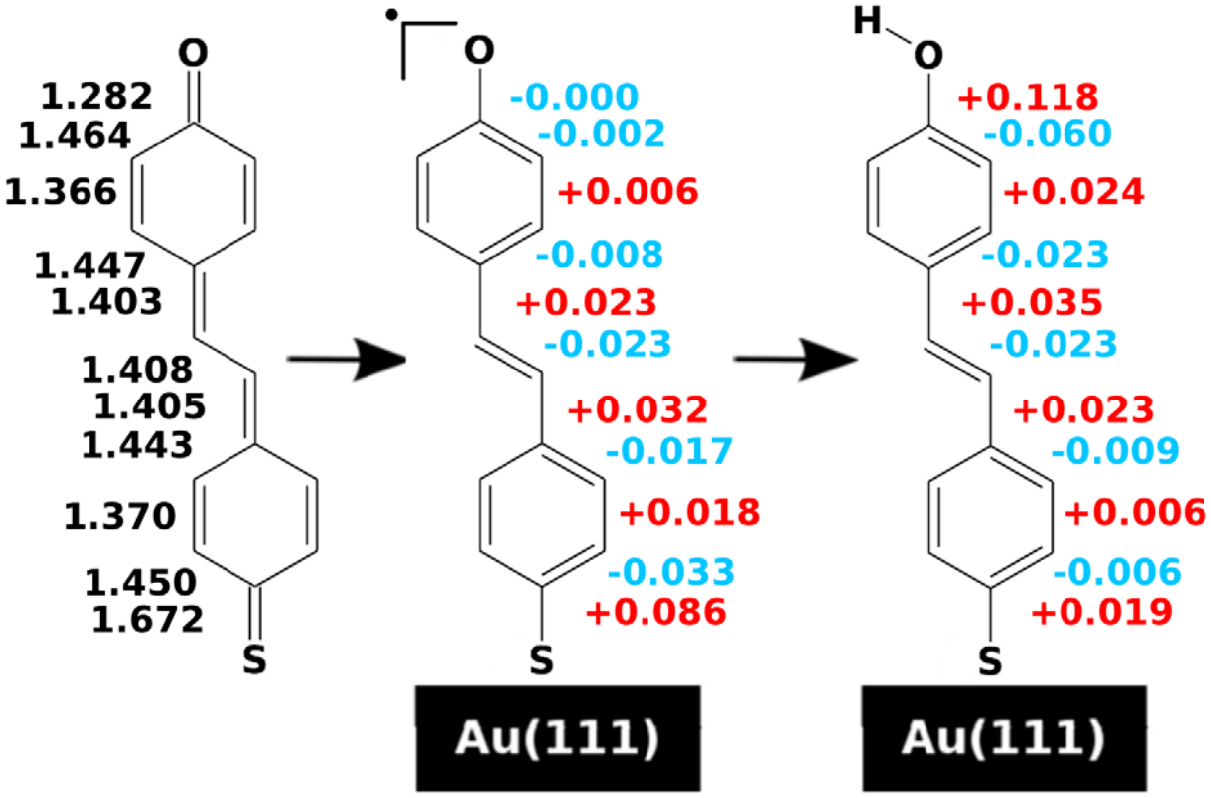

Fig. S4. Bond length changes upon adsorption of 1 on the Au(111) surface, and upon subsequent reduction.

This journal is © The Royal Society of Chemistry 2012

References:

1. G. Kresse and J. Furthmüller, *Phys. Rev. B*, 1996, **54**, 11169-11186.
2. G. Kresse and D. Joubert, *Phys. Rev. B*, 1999, **59**, 1758-1775.
3. P. Blöchl, *Phys. Rev. B*, 1994, **50**, 17953-17979.
4. H. Monkhorst and J. Pack, *Phys. Rev. B*, 1976, **13**, 5188-5192.
5. G. Heimel, L. Romaner, J. Brédas, and E. Zojer, *Surf. Sci.*, 2006, **600**, 4548-4562.
6. A. Kokalj, *Comput. Mater. Sci.*, 2003, **28**, 155-168.
7. S. Grimme, *J. Comput. Chem.*, 2006, **27**, 1787-1799.
8. A. Tkatchenko and M. Scheffler, *Phys. Rev. Lett.*, 2009, **102**, 073005.
9. S. Kümmel and L. Kronik, *Rev. Mod. Phys.*, 2008, **80**, 3-60.
10. F. Rissner, D. A. Egger, A. Natan, T. Körzdörfer, S. Kümmel, L. Kronik, and E. Zojer, *J. Am. Chem. Soc.*, 2011, 110929034013009.
11. J. Neaton, M. Hybertsen, and S. Louie, *Phys. Rev. Lett.*, 2006, **97**, 216405.
12. J. M. Garcia-Lastra, C. Rostgaard, A. Rubio, and K. S. Thygesen, *Phys. Rev. B*, 2009, **80**, 245427.
13. A. Biller, I. Tamblyn, J. B. Neaton, and L. Kronik, *J. Chem. Phys.*, 2011, **135**, 164706.
14. T. Körzdörfer, S. Kümmel, N. Marom, and L. Kronik, *Phys. Rev. B*, 2009, **79**, 201205.